Neutron Production from Ultrathin Foils by Radiation Pressure driven Ions

Contact: s.kar@qub.ac.uk

A. Alejo, S. Kar, H. Ahmed, A. Green, D. Jung, M. Zepf, M. Borghesi
Centre for Plasma Physics, School of Mathematics and Physics, Queen's University Belfast, BT7 1NN, UK

A.G. Krygier, R.R. Freeman
Department of Physics, The Ohio State University, Columbus, Ohio 43210, USA

J.T. Morrison
Propulsion Systems Directorate, Air Force Research Lab, Wright Patterson Air Force Base, Ohio 45433, USA

R. Clarke, J.S. Green, P. Norreys*, M. Notley
Central Laser Facility, Rutherford Appleton Laboratory, Didcot, Oxfordshire, OX11 0QX, UK

M. Oliver
*Department of Physics, University of Oxford, Oxford, OX1 3PU, UK

J. Fuchs, L. Vassura
LULI, Ecole Polytechnique, CNRS, Palaiseau Cedex, 91128, France

A. Kleinschmidt, M. Roth
Institut für Kernphysik, Technische Universität Darmstadt, Schloßgartenstrasse 9, D-64289 Darmstadt, Germany

Z. Najmudin, H. Nakamura
Blackett Laboratory, Department of Physics, Imperial College London, SW7 2AZ, UK

1 Introduction

An ultra-short burst of fast neutrons would have a wide range of applications in science [1], industry [2,3], security [4] or healthcare [5]. However, the reduced number of large neutron facilities and the limitations in their access has led to an increasing interest in developing table-top sources. Laser-driven ion accelerators have been investigated as a possible solution [6–9], with advantages such as compactness, cost-effectiveness and improved radiation confinement. Such neutron sources are mainly based on the use of ions accelerated via the Target-Normal Sheath Acceleration mechanism (TNSA) [10–13] impinging on suitable neutron converter targets. However, despite of being a robust mechanism, TNSA presents a number of limitations, such as a slow ion-energy scaling with respect to the incident laser intensity ($E_{ion} \propto \sqrt{I_L}$), or a divergent beam predominantly formed by protons, which largely reduce the range of possible nuclear reactions involved in the neutron generation. Significant attention is therefore being given to the exploration of other promising acceleration mechanisms, such as Radiation Pressure Acceleration (RPA) [14–20] or Break-Out Afterburner (BOA) [21–25], by taking advantage of the high laser intensity (beyond 10^{20} W cm^{-2}) currently accessible.

Of particular interest is the Light Sail regime of RPA, in which the laser is capable of detaching the irradiated region of an ultra-thin target, leading to efficient acceleration of all ion species in the target in a narrow spectral bandwidth and divergence cone. Recent experimental data [20] and extensive particle-in-cell simulations [14, 16, 19] indicate a fast ion energy scaling ($E_{ion} \propto (a_0^2 \tau_p / \chi)^2$, where $a_0^2 \tau_p$ and χ represent incident laser fluence on the target and target areal density respectively in dimensionless units) in this regime of accel-

eration, which extrapolates to ion energies beyond 100s of MeV/amu [26, 27] with upcoming laser facilities [28]. A key requirement of this approach is to maintain the integrity of ultra-thin targets over the duration of the laser pulse. Where the RPA mechanism relies on the reflection of light from a moving object , use of low areal mass targets to achieve higher ion energy poses a significant challenge in preventing transparency. For an ultra-thin slab of plasma this can happen due to a combination of volumetric target heating and premature expansion, as well as self-induced relativistic transparency (SIT) [29, 30] - a regime where the laser propagates through the foil due to insufficient shielding offered by the relativistically increasing inertia of the electrons in an intense laser field.

Here we report on the study of neutron generation by RPA-driven ions. The onset of RPA-LS mechanism for ultrathin (sub-micron thick) deuterated plastic foils was identified not only by the appearance of narrow-bandwidth features in the deuteron spectra, but also by an abrupt increase in neutron flux and energy. Since the neutrons' flux, angular distribution and spectrum solely depend on the density, energy and divergence of the ions producing them, neutron spectroscopy can provide information about their parent ions. This information, which is extremely difficult otherwise to obtain, underpins any issues with stability and efficiency of the LS-RPA mechanism and hence, facilitates optimising the production process for both ions and neutrons.

2 Experimental Setup

The experiment was carried out at the Rutherford Appleton Laboratory (RAL), STFC, UK by employing the petawatt arm of the VULCAN laser (wavelength (λ)=1053nm) system [31]. A schematic of the experi-
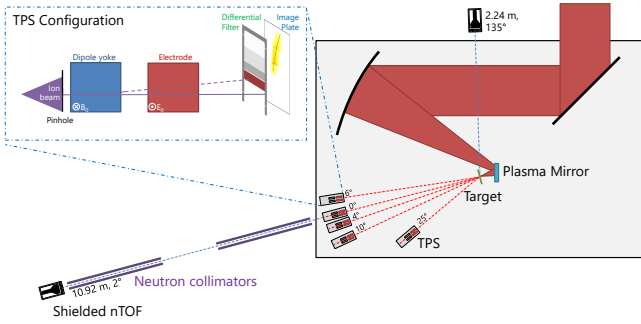
Figure 1: *(a) Experimental setup, showing the angularly distributed Thomson Parabola Spectrometers (TPS) and neutron scintillators. The inset represents the placing of the differential filter inside each TPS for species discrimination.*

mental setup is shown in Fig. 1, where the laser is focussed on the target foil at normal incidence by an $f/3$ parabola down to a ~ 5 μm spot (Full Width at Half Maximum) after being reflected from a plasma mirror [32], achieving a contrast ratio between the main pulse and the nanosecond-long amplified spontaneous emission of $\sim 10^9$. The laser delivered $100 - 250$ J on the target in 850 ± 150 fs pulses, leading to a peak intensity (I_0) on the target in the range 1×10^{20} $-$ 3×10^{20} W cm^{-2}. The targets were made of deuterated plastic ($(C_2D_4)_n$, henceforth referred as CD) with thickness in the range $l = 90 - 900$ nm and 10μm. The ions produced from the target were diagnosed using five Thomson Parabola Spectrometers (TPS) [33, 34] looking at -6 deg, 0 deg, 4 deg, 10 deg and 25 deg with respect to the laser axis (which coincides with the target normal due to the normal incidence). Due to the overlapping traces of other ion species with similar charge-to mass ratios, such as C^{6+} or O^{8+}, a differential filtering technique [35] was implemented to obtain the full energy spectrum of deuterons in each TPS. The neutrons generated from the laser irradiated target were diagnosed along the laser axis and at ~ 135 deg off the laser axis by using fast plastic scintillator (EJ232Q) detectors in time-of-flight (nToF) configuration. The on- and off-axis nToF detectors were placed at the farthest possible distance(10.9 m and 2.2 m, respectively) from the target and were shielded against Bremsstrahlung and γ radiation produced from the interaction by using $5 - 10$ cm of lead surrounding the detectors. Where the energy of the neutrons revealed by the detector is obtained by their time-of-flight, the neutron flux was obtained by cross-calibrating the detectors with absolutely calibrated Bubble Detector Spectrometers (BDS) as discussed in [36].

3 Deuterium acceleration via RPA-LS

Most of the efforts regarding the generation of a bright, directional neutron beam have been focussed on the use

of a pitcher-catcher configuration, in which the laser-driven ions impinge onto a secondary target, where the nuclear reactions take place. The need of such double-target setup arises from the fact that direct laser irradiation of single targets with thickness $> $ μm typically generated neutrons isotropically and with low flux. The aim of our experiments was to extend this single target studies to the ultrathin range, and obtain information on the laser interaction and acceleration process from the combined and simultaneous diagnosis of neutrons and ions.

As expected from the TNSA mechanism, quasi-exponential ion spectra were obtained from the irradiation of thick targets (10μm) as shown in Fig. 2(a). Since the TNSA mechanism favours acceleration of highest charge-to-mass ratio ion species (in our case protons, abundantly supplied by the hydrocarbon contamination layer present on the target surface), inefficient acceleration of the deuterium ions (up to a maximum energy of ~ 5 MeV/nucleon) was observed in this case. However, when the target thickness was reduced to a few hundreds of nanometres, narrow-bandwidth spectral features appeared towards the high energy end of the deuteron spectra, with significant increase in cut-off energy (for instance, see Fig. 2(a) for the deuteron spectra obtained from 320 nm or 400 nm targets). Furthermore, this high energy component in the deuteron beam was observed to be contained within a narrow angular cone along the laser axis. Such ion spectral behaviour from ultra-thin targets has been previously reported by Kar *et al.* [20], attributing it to the onset of RPA-LS mechanism in a TNSA hybrid regime. Here the spectral peaks are observed for a bulk species of the target, in contrast to [20], where the observations referred to carbon ions from the contamination layer.

The energy of the features appearing on both the proton and deuteron spectra was obtained over a number of shots by varying the target thickness in the range 900 nm to 90 nm. For target thickness above 320 nm, the peaks in proton and deuteron spectra were found to be in a good agreement with the expected scaling of RPA-LS mechanism [20] , as shown in the Fig. 2(b). The energies at the spectral peaks for the deuterons were slightly lower than those for the protons, as expected in a multi-species scenario [20]. However, for target thickness below 320 nm, the energy of the bunches fell below the expected energy from LS scaling, in coincidence with a broadening of the spectral peaks, and the appearance of a plateau at the high energies, as shown for the 90 nm target in Fig. 2(a).

4 Neutron generation

While using deuterated plastic target to study the bulk ion acceleration in the RPA-LS regime, diagnosing neutron emission at the same time provides an unique insight in the acceleration phase. A comparison between
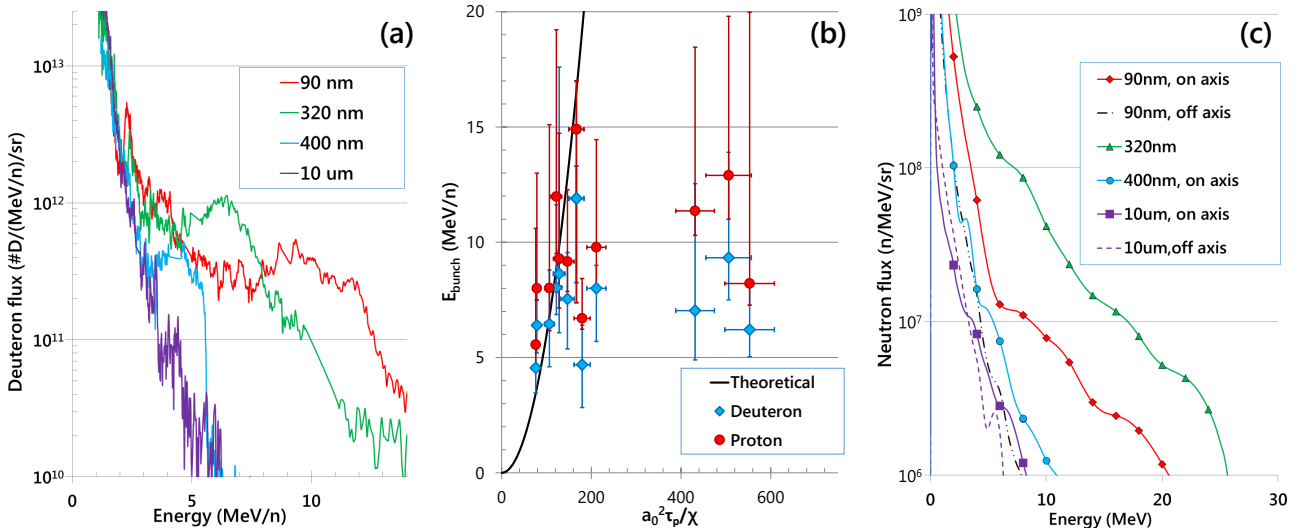
2

Figure 2: *(a) Appearance of narrow-bandwidth features in the deuterium spectra. (b) Scaling of the bunch energy depending on laser and target parameters for both proton and deuterium ions, compared to the theoretical curve [20].(c) Variation of the neutron spectrum depending on the target thickness.*

the neutron spectra obtained for different target thickness is shown in Fig. 2(c).

For the thick targets (10μm), where the ions are mainly driven by the TNSA mechanism with an exponential energy spectra and large divergence (see fig. 2(a)), an isotropic, low-flux neutron emission was measured. In this case the neutrons are most likely produced at the target front surface, either from the thermonuclear reactions in the hot dense plasma produced by the laser interaction, or by the ions driven by the hole-boring mechanism into the the bulk of the target [6]. As the thickness of the target was reduced to 320 nm, a substantial increase in neutron generation was observed, as shown in the Fig. 2(c). In this case, the neutron emission along the laser forward direction has significantly higher neutron flux and energy than what observed in the laser off-axis detector, where no significant differences are detected from the 10μm thick target case. Since the CD targets were irradiated without any other object in the vicinity along the laser forward direction (the closest object was the TPS at a distance of ∼1.5 m away from the target), we can confidently assume that the observed neutrons are generated primarily from the laser irradiated target by d(d,n)^{3}He reaction. A further reduction of the target thickness to 90 nm led to a large drop in the neutron flux. It is interesting to note here that the reduction in neutron flux does not correlate with the parent-ion flux, implying that this difference must relate to different conditions during the ion acceleration.

In order to explain the increase in flux when the RPA range is approached, as well as the eventual drop, a plasma cylinder model can be considered, in which neu-

tron yield is given by

$$Y_n \simeq \frac{\tau_{burn}}{2} \int n_d^2 \langle \sigma v \rangle \ dV \qquad (1)$$

where, n_d is the deuteron number density interacting for an interval τ_{burn}, the fusion burn time, and $\langle \sigma v \rangle$ is the velocity averaged fusion reactivity. In Light Sail , the accelerated ions propagate together as a dense bunch for a significant length of time, which can make the beam plasma fusion described above an efficient process. If the target is too thin, however, self-induced transparency takes place, which typically leads to broader spectra associated to electron heating rather than radiation pressure effects. In this case the possibility for the ions to interact with each other within a dense bunch over an extended time is removed, when the target is too thin, would cause the disappearance of the spectral bunch, as observed in the 90 mm case of Fig.2 (c).

5 Conclusions

The cohesive acceleration of ion bunches during the LS phase is underpinned implicitly by the observed increase in neutron flux and anisotropy, as well as by the observation of an abrupt drop in neutron generation for sufficiently thin targets, which are likely to become relativistically transparent during the interaction. Therefore, neutron spectroscopy proved to be an useful diagnostic for understanding and optimising the ion acceleration mechanism. The data also show that neutron generation from LS-driven ion bunches is an efficient route to produce a compact laser-driven neutron source, alternative to more conventionally used pitcher-catcher methods.

References

[1] Higginson, D. P. et al., Phys. Plasmas **17** (2010) 100701.

[2] Perkins, L. et al., Nuclear Fusion **40** (2000) 1.

[3] Nakai, S., J. of Phys., Conf. Series **112** (2008) 042070.

[4] Loveman, R., Bendahan, J., Gozani, T., and Stevenson, J., Nucl. Instru. Methods B **99** (1995) 765 .

[5] Wittig, A. et al., Crit. Rev. Oncology/Hematology **68** (2008) 66.

[6] Norreys, P. et al., Plasma physics and controlled fusion **40** (1998) 175.

[7] Lancaster, K. et al., Physics of plasmas **11** (2004) 3404.

[8] Willingale, L. et al., Physics of Plasmas **18** (2011) 083106.

[9] Zulick, C. et al., Applied Physics Letters **102** (2013) 124101.

[10] Wilks, S. et al., Physics of Plasmas **8** (2001) 542.

[11] Fuchs, J. et al., Nature Physics **2** (2005) 48.

[12] Robson, L. et al., Nature Physics **3** (2006) 58.

[13] Passoni, M., Bertagna, L., and Zani, A., New Journal of Physics **12** (2010) 045012.

[14] Esirkepov, T., Borghesi, M., Bulanov, S., Mourou, G., and Tajima, T., Physical Review Letters **92** (2004) 175003.

[15] Kar, S. et al., Physical Review Letters **100** (2008) 225004.

[16] Robinson, A., Zepf, M., Kar, S., Evans, R., and Bellei, C., New Journal of Physics **10** (2008) 013021.

[17] Robinson, A. et al., Plasma Physics and Controlled Fusion **51** (2009) 024004.

[18] Macchi, A., Veghini, S., Liseykina, T. V., and Pegoraro, F., New Journal of Physics **12** (2010) 045013.

[19] Qiao, B. et al., Physical Review Letters **108** (2012) 115002.

[20] Kar, S. et al., Physical Review Letters **109** (2012) 185006.

[21] Yin, L. et al., Physics of plasmas **14** (2007) 056706.

[22] Yin, L. et al., Physical Review Letters **107** (2011) 045003.

[23] Jung, D. et al., Physical Review Letters **107** (2011) 115002.

[24] B. Hegelich, "Towards GeV laser-driven ion acceleration", Towards gev laser-driven ion acceleration, in *Coulomb 2009, Senigallia, Italy*, 2009.

[25] Jung, D. et al., New Journal of Physics **15** (2013) 123035.

[26] Qiao, B., Zepf, M., Borghesi, M., and Geissler, M., Physical review letters **102** (2009) 145002.

[27] Bulanov, S. et al., Phys. Rev. Lett. **114** (2015) 105003.

[28] Extreme light infraestracture(eli), `http://www.eli-np.ro//`.

[29] Kaw, P. and Dawson, J., Physics of Fluids (1958-1988) **13** (1970) 472.

[30] Guerin, S., Mora, P., Adam, J., Héron, A., and Laval, G., Physics of Plasmas (1994-present) **3** (1996) 2693.

[31] Danson, C. et al., Nuclear Fusion **44** (2004) S239.

[32] Thaury, C. et al., Nature Physics **3** (2007) 424.

[33] Thomson, J. J., Proceedings of the Royal Society of London. Series A **89** (1913) 1.

[34] Gwynne, D. et al., Review of Scientific Instruments **85** (2014).

[35] Alejo, A. et al., Review of Scientific Instruments **85** (2014).

[36] Mirfayzi, S. et al., Review of Scientific Instruments **86** (2015).